



MOTECUSOMA

MONITORING THE ENERGY CYCLE FOR A BETTER UNDERSTANDING OF CLIMATE CHANGE

CCI CROSS-ECV PROJECT

SCIENCE REQUIREMENTS DOCUMENT

	Name	Organisation	Date	Visa
Written by :	Consortium	Magellium	06/01/2025	
Checked by :	Michaël Ablain	Magellium	06/01/2025	
Approved by :	Joël Dorandeu	Magellium	06/01/2025	
Accepted by:	Sarah Connors	ESA		

Document reference :	MOTECUSOMA-DT-004-MAG_SRD_D1.1
Edition.Revision :	1.1
Date Issued:	04/04/2025
Customer :	ESA
Ref. Market, consultation :	ESA/AO/1-12062/23/I-NB

Distribution List

	Name	Organisation	No. copies
Sent to :	Sarah Connors	ESA	1 (digital copy)
Internal copy :	Project folder	Magellium	1 (digital copy)

Document evolution sheet

Ed.	Rev.	Date	Purpose evolution	Comments
1	0	23/10/2024	Creation of document	
1	1	06/01/2024	ESA feedbacks	

Contents

1. Introduction	5
1.1. Scope and objective	5
1.2. Document structure	5
1.3. Related documents	5
1.3.1. Applicable documents	5
1.3.2. References	5
1.4. Acronyms	7
2. Overall science requirements	9
2.1. Scientific Challenges and Requirements in Understanding Earth's Energy Cycle	9
2.2. The Earth's Energy Budget	9
2.3. Rising Energy Imbalance: Current Trends and Challenges	9
2.4. Feedback Mechanisms and Climate Sensitivity	10
2.5. Scientific Challenges Ahead	11
2.6. Conclusion	11
3. Requirements for the Earth Energy Imbalance (EEI)	12
3.1. Summary of Hakuba et al. (2024)	12
3.2. Requirements	13
4. Requirements for the Surface Air Temperature (TAS)	14
4.1. Introduction: Surface Temperatures	14
4.1.1. Required form of surface temperature	14
4.1.2. General requirements on satellite-derived TAS	17
4.2. Science Requirements for Marine TAS	18
4.2.1. Open-ocean marine air temperature	18
4.2.2. Air temperature over high sea-ice concentrations	20
4.2.3. Marginal ice zones: sea-ice/water mixtures	21
4.3. Science Requirements for Land TAS	22
4.3.1. Surface air temperature over land and lakes	22
4.3.2. Surface air temperature over ice sheets and shelves	23
4.4. Science Requirements for TAS Analysis	25
4.4.1. Single domain L3 non-interpolated TAS estimates	25
4.4.2. Merged multi-domain L4 interpolated TAS estimates	26

List of figures and tables

Figure 1: Different surface temperatures. SST: sea surface temperature, either at depth, measured in situ, or of the skin layer, measured by radiometers on ships or in space; MAT: marine air temperature; LST: land surface temperature, LSAT: land surface air temperature; LSWT: lake surface water temperature; IST: ice surface temperature, which covers land-ice and ice shelves, and SIST for sea-ice surface temperature.	19
Figure 2: Correlation coefficient between monthly mean surface temperature and mid-tropospheric temperature (500 hPa) for (left) Januarys and (right) Julys over the period 1980 to 2024. (Upper) correlation of skin ST and mid-tropospheric temperature, and (lower) 2 m air temperature (TAS) and the same.	20
Figure 3: Correlation between monthly zonal-mean surface and mid-tropospheric temperatures, for Januarys (left) and Julys (right).	21
Figure 4: Mean difference of Tmax from Tmean for (left) January and (right) July.	21
Figure 5: As Figure 2, but for the Tmax rather than Tmean representation of TAS.	22
Table 1: List of applicable documents.	7
Table 2: List of abbreviations and acronyms.	10
Table 3: Science requirements for EEI	16

1. Introduction

1.1. Scope and objective

This document is the Science Requirements Document (SRD) for the ESA MOTECUSOMA project ([AD-1] and [AD-2]). It aims at providing a detailed review of the knowledge gaps and science requirements for all the components of the energy cycle foreseen at the beginning of the project and that will be the basis for the development of EEI and TAS products.

1.2. Document structure

In addition to this introduction, the document is organised as follows:

- Section 2: Overall Science Requirement
- Section 3: Requirements for the earth energy Imbalance
- Section 4: Requirements for the surface Air Temperature

1.3. Related documents

1.3.1. Applicable documents

Table 1 *List of applicable documents.*

Id.	Ref.	Description
[AD1]		ESA-EOP-SC-AMT-2023-21 : Call to tender CLIMATE-SPACE - THEME II: CROSS-ECV ACTIVITIES
[AD2]	MAG-24-PTF-023	Detailed MAGELLIUM offer in response to ESA/ECSAT Request for Quotation "CCI CROSS ECV" AO/1-12062/23/I-NB

1.3.2. References

- Biri, S., Cornes, R. C., Berry, D. I., Kent, E. C., and Yelland, M. J.: AirSeaFluxCode: Open-source software for calculating turbulent air-sea fluxes from meteorological parameters, *Front. Mar. Sci.*, 9, 2023.
- Cornes, R. C., Kent, Elizabeth. C., Berry, David. I., and Kennedy, J. J.: CLASSnmat: A global night marine air temperature data set, 1880–2019, *Geosci. Data J.*, 7, 170–184, <https://doi.org/10.1002/gdj3.100>, 2020.
- Cropper, T. E., Berry, D. I., Cornes, R. C., and Kent, E. C.: Quantifying Daytime Heating Biases in Marine Air Temperature Observations from Ships, *J. Atmospheric Ocean. Technol.*, 40, 427–438, <https://doi.org/10.1175/JTECH-D-22-0080.1>, 2023.

- Forster, P., Storelvmo, T., Armour, K., Collins, W., Dufresne, J.-L., Frame, D., Lunt, D., Mauritsen, T., Palmer, M., and Watanabe, M.: The Earth's energy budget, climate feedbacks, and climate sensitivity, 2021.
- Hakuba, M. Z., Fourest, S., Boyer, T., Meyssignac, B., Carton, J. A., Forget, G., Cheng, L., Giglio, D., Johnson, G. C., Kato, S., Killick, R. E., Kolodziejczyk, N., Kuusela, M., Landerer, F., Llovel, W., Locarnini, R., Loeb, N., Lyman, J. M., Mishonov, A., Pilewskie, P., Reagan, J., Storto, A., Sukianto, T., and Von Schuckmann, K.: Trends and Variability in Earth's Energy Imbalance and Ocean Heat Uptake Since 2005, *Surv. Geophys.*, <https://doi.org/10.1007/s10712-024-09849-5>, 2024.
- Huang, B., Menne, M. J., Boyer, T., Freeman, E., Gleason, B. E., Lawrimore, J. H., Liu, C., Rennie, J. J., Schreck, C. J., Sun, F., Vose, R., Williams, C. N., Yin, X., and Zhang, H.-M.: Uncertainty Estimates for Sea Surface Temperature and Land Surface Air Temperature in NOAA GlobalTemp Version 5, *J. Clim.*, 33, 1351–1379, <https://doi.org/10.1175/JCLI-D-19-0395.1>, 2020.
- Kent, E. C., Rayner, N. A., Berry, D. I., Saunby, M., Moat, B. I., Kennedy, J. J., and Parker, D. E.: Global analysis of night marine air temperature and its uncertainty since 1880: The HadNMAT2 data set, *J. Geophys. Res. Atmospheres*, 118, 1281–1298, <https://doi.org/10.1002/jgrd.50152>, 2013.
- Lenssen, N., Schmidt, G. A., Hendrickson, M., Jacobs, P., Menne, M. J., and Ruedy, R.: A NASA GISTEMPv4 Observational Uncertainty Ensemble, *J. Geophys. Res. Atmospheres*, 129, e2023JD040179, <https://doi.org/10.1029/2023JD040179>, 2024.
- Lindgren, F., Rue, H., and Lindström, J.: An Explicit Link between Gaussian Fields and Gaussian Markov Random Fields: The Stochastic Partial Differential Equation Approach, *J. R. Stat. Soc. Ser. B Stat. Methodol.*, 73, 423–498, <https://doi.org/10.1111/j.1467-9868.2011.00777.x>, 2011.
- Loeb, N. G., Doelling, D. R., Wang, H., Su, W., Nguyen, C., Corbett, J. G., Liang, L., Mitrescu, C., Rose, F. G., and Kato, S.: Clouds and the Earth's Radiant Energy System (CERES) Energy Balanced and Filled (EBAF) Top-of-Atmosphere (TOA) Edition-4.0 Data Product, *J. Clim.*, 31, 895–918, <https://doi.org/10.1175/JCLI-D-17-0208.1>, 2018.
- Loeb, N. G., Ham, S.-H., Allan, R. P., Thorsen, T. J., Meyssignac, B., Kato, S., Johnson, G. C., and Lyman, J. M.: Observational Assessment of Changes in Earth's Energy Imbalance Since 2000, *Surv. Geophys.*, 45, 1757–1783, <https://doi.org/10.1007/s10712-024-09838-8>, 2024.
- Merchant, C. J., Matthiesen, S., Rayner, N. A., Remedios, J. J., Jones, P. D., Olesen, F., Trewin, B., Thorne, P. W., Auchmann, R., Corlett, G. K., Guillevic, P. C., and Hulley, G. C.: The surface temperatures of Earth: steps towards integrated understanding of variability and change, *Geosci. Instrum. Methods Data Syst.*, 2, 305–321, <https://doi.org/10.5194/gi-2-305-2013>, 2013.
- Merchant, C. J., Holl, G., Mittaz, J. P. D., and Woolliams, E. R.: Radiance Uncertainty Characterisation to Facilitate Climate Data Record Creation, *Remote Sens.*, 11, 474, <https://doi.org/10.3390/rs11050474>, 2019.
- Meyssignac, B., Boyer, T., Zhao, Z., Hakuba, M. Z., Landerer, F. W., Stammer, D., Köhl, A., Kato, S., L'Ecuyer, T., Ablain, M., Abraham, J. P., Blazquez, A., Cazenave, A., Church, J. A., Cowley, R., Cheng, L., Domingues, C. M., Giglio, D., Gouretski, V., Ishii, M., Johnson, G. C., Killick, R. E., Legler, D., Llovel, W., Lyman, J., Palmer, M. D., Piotrowicz, S., Purkey, S. G., Roemmich, D., Roca, R., Savita, A., Schuckmann, K. von, Speich, S., Stephens, G., Wang, G., Wijffels, S. E., and Zilberman, N.: Measuring Global Ocean Heat Content to Estimate the Earth Energy Imbalance, *Front. Mar. Sci.*, 6, <https://doi.org/10.3389/fmars.2019.00432>, 2019.

- Minobe, S., Behrens, E., Findell, K. L., Loeb, N. G., Meyssignac, B., and Sutton, R.: Global and Regional Drivers for Exceptional Climate Extremes in 2023-2024: Beyond the New Normal, <https://doi.org/10.21203/rs.3.rs-5454786/v1>, 14 November 2024.
- Mittaz, J., Merchant, C. J., and Woolliams, E. R.: Applying principles of metrology to historical Earth observations from satellites, *Metrologia*, 56, 032002, <https://doi.org/10.1088/1681-7575/ab1705>, 2019.
- Morice, C. P., Kennedy, J. J., Rayner, N. A., Winn, J. P., Hogan, E., Killick, R. E., Dunn, R. J. H., Osborn, T. J., Jones, P. D., and Simpson, I. R.: An Updated Assessment of Near-Surface Temperature Change From 1850: The HadCRUT5 Data Set, *J. Geophys. Res. Atmospheres*, 126, e2019JD032361, <https://doi.org/10.1029/2019JD032361>, 2021.
- Morice, C. P., Berry, D. I., Cornes, R. C., Cowtan, K., Cropper, T., Hawkins, E., Kennedy, J. J., Osborn, T. J., Rayner, N. A., Rivas, B. R., Schurer, A. P., Taylor, M., Teleti, P. R., Wallis, E. J., Winn, J., and Kent, E. C.: An observational record of global gridded near surface air temperature change over land and ocean from 1781, <https://doi.org/10.5194/essd-2024-500>, 5 December 2024.
- Nielsen-Englyst, P., Høyer, J. L., Kolbe, W. M., Dybkjær, G., Lavergne, T., Tonboe, R. T., Skarpalezos, S., and Karagali, I.: A combined sea and sea-ice surface temperature climate dataset of the Arctic, 1982–2021, *Remote Sens. Environ.*, 284, 113331, <https://doi.org/10.1016/j.rse.2022.113331>, 2023.
- Rayner, N. A., Auchmann, R., Bessembinder, J., Brönnimann, S., Brugnara, Y., Capponi, F., Carrea, L., Dodd, E. M. A., Ghent, D., Good, E., Høyer, J. L., Kennedy, J. J., Kent, E. C., Killick, R. E., Van Der Linden, P., Lindgren, F., Madsen, K. S., Merchant, C. J., Mitchelson, J. R., Morice, C. P., Nielsen-Englyst, P., Ortiz, P. F., Remedios, J. J., Van Der Schrier, G., Squintu, A. A., Stephens, A., Thorne, P. W., Tonboe, R. T., Trent, T., Veal, K. L., Waterfall, A. M., Winfield, K., Winn, J., and Woolway, R. I.: The EUSTACE Project: Delivering Global, Daily Information on Surface Air Temperature, *Bull. Am. Meteorol. Soc.*, 101, E1924–E1947, <https://doi.org/10.1175/BAMS-D-19-0095.1>, 2020.
- Rugenstein, M., Zelinka, M., Karnauskas, K., Ceppi, P., and Andrews, T.: Patterns of Surface Warming Matter for Climate Sensitivity, *Eos*, 104, <https://doi.org/10.1029/2023EO230411>, 2023.
- von Schuckmann, K., Minière, A., Gues, F., Cuesta-Valero, F. J., Kirchengast, G., Adusumilli, S., Straneo, F., Ablain, M., Allan, R. P., Barker, P. M., Beltrami, H., Blazquez, A., Boyer, T., Cheng, L., Church, J., Desbruyeres, D., Dolman, H., Domingues, C. M., García-García, A., Giglio, D., Gilson, J. E., Gorfer, M., Haimberger, L., Hakuba, M. Z., Hendricks, S., Hosoda, S., Johnson, G. C., Killick, R., King, B., Kolodziejczyk, N., Korosov, A., Krinner, G., Kuusela, M., Landerer, F. W., Langer, M., Lavergne, T., Lawrence, I., Li, Y., Lyman, J., Marti, F., Marzeion, B., Mayer, M., MacDougall, A. H., McDougall, T., Monselesan, D. P., Nitzbon, J., Otosaka, I., Peng, J., Purkey, S., Roemmich, D., Sato, K., Sato, K., Savita, A., Schweiger, A., Shepherd, A., Seneviratne, S. I., Simons, L., Slater, D. A., Slater, T., Steiner, A. K., Suga, T., Szekely, T., Thiery, W., Timmermans, M.-L., Vanderkelen, I., Wjiffels, S. E., Wu, T., and Zemp, M.: Heat stored in the Earth system 1960–2020: where does the energy go?, *Earth Syst. Sci. Data*, 15, 1675–1709, <https://doi.org/10.5194/essd-15-1675-2023>, 2023.
- Stephens, G., Polcher, J., Zeng, X., Oevelen, P. van, Poveda, G., Bosilovich, M., Ahn, M.-H., Balsamo, G., Duan, Q., Hegerl, G., Jakob, C., Lamptey, B., Leung, R., Piles, M., Su, Z., Dirmeyer, P., Findell, K. L., Verhoef, A., Ek, M., L’Ecuyer, T., Roca, R., Nazemi, A., Dominguez, F., Klocke, D., and Bony, S.: The First 30 Years of GEWEX, *Bull. Am.*

Meteorol. Soc., 104, E126–E157, <https://doi.org/10.1175/BAMS-D-22-0061.1>, 2023.

1.4. Acronyms

Table 2 *List of acronyms.*

Acronym	Description
EEI	Earth Energy Imbalance
GEWEX	Global Energy and Water Exchanges
GHG	GreenHouse Gas
IMS	Ice Mapping System
LSAT	Land Surface Air Temperature
MAT	Marine Air Temperatures
NSIDC	National Snow and Ice data Center
OHC	Ocean Heat Content
OLR	Outgoing Longwave Radiation
RF	Radiative Forcing
ST	Surface Temperature
TAS	Surface Air Temperature

2. Overall science requirements

2.1. Scientific Challenges and Requirements in Understanding Earth's Energy Cycle

The key challenge of climate change lies in understanding how the Sun's energy is distributed, stored, and reflected/re-emitted by Earth. Human-induced climate forcing—mainly from greenhouse gas (GHG) emissions and aerosols—has disrupted the balance between absorbed solar radiation and outgoing thermal radiation, leading to global warming. This imbalance, known as the Earth Energy Imbalance (EEI), is central to understanding the climate system and its response to anthropogenic activities.

Historically, climate scientists have sought to understand the fate of solar energy absorbed by Earth and how it fuels the global energy cycle. Pioneering studies by Fourier (1824), Arrhenius (1896), and others laid the foundation for modern climate science. Scientific interest intensified in the mid-20th century as evidence grew of GHGs' role in amplifying the greenhouse effect and altering Earth's energy flows. In response, the Global Energy and Water Exchanges (GEWEX) program was launched in 1990 under the World Climate Research Program. Its aim was to bridge gaps in understanding Earth's water and energy cycles using advanced satellite observations and climate models. Over the past three decades, this initiative has dramatically improved our ability to quantify and predict the processes involved in Earth's water energy cycle, although key challenges remain (Stephens et al., 2023).

2.2. The Earth's Energy Budget

Earth receives approximately 340 W/m^2 of solar radiation, predominantly in the visible spectrum. Of this, 70.5% is absorbed by the surface and atmosphere, while the remaining 29.5% is reflected back to space by clouds, aerosols, and surface albedo. The absorbed energy heats the planet, and in turn, Earth emits infrared radiation to space. Some of this outgoing longwave radiation (OLR) is absorbed and re-emitted by GHGs in the atmosphere, trapping heat and further warming the surface—a process known as the greenhouse effect.

Currently, Earth emits around 239.5 W/m^2 of OLR to space. The slight difference between absorbed solar energy ($\sim 240 \text{ W/m}^2$) and emitted infrared radiation ($\sim 239.5 \text{ W/m}^2$) creates a persistent positive radiation imbalance of approximately 0.5 to 1 W/m^2 , which drives global warming. This imbalance is mostly the result of increased GHG concentrations reducing Earth's ability to emit energy to space. The EEI, while small in absolute magnitude, represents a critical driver of rising temperatures, sea-level rise, and other climate impacts.

2.3. Rising Energy Imbalance: Current Trends and Challenges

The EEI reflects a combination of anthropogenic forcing, feedback mechanisms, and natural variability. While GHGs drive the long-term increase in EEI by trapping heat, aerosols offset some of this warming by reflecting sunlight. However, aerosol cooling effects are weakening due to improved air quality policies. Feedbacks such as increased outgoing infrared radiation (negative feedback) and enhanced water vapor concentrations (positive feedback) play a crucial role in modulating the EEI. Additionally, natural phenomena like El Niño events introduce year-to-year fluctuations in the energy balance.

Recent observations indicate that the EEI has been increasing faster than expected, reaching 1.8 W/m^2 in 2023, more than double its value two decades earlier. This trend is difficult to reconcile with current climate models, which struggle to replicate the observed rate of change. Factors contributing to this discrepancy may include misrepresented sea surface temperature patterns, inaccurate aerosol emission estimates, or poorly understood feedback processes. These results have been published in 2 papers Loeb et al. (2024) and Mauritsen et al. (in revision). The record-breaking surface temperatures in 2023 and early 2024 highlight the urgent need to disentangle the underlying causes of these changes. Observing trends in both emitted infrared and reflected solar radiation is critical for understanding how energy flows through the climate system. These results are published in the paper Minobe et al. (2024). However, these observations depend heavily on satellite instruments like NASA's CERES and TSIS, many of which are nearing the end of their operational lifetimes. The lack of continuity in satellite missions poses a severe risk to our ability to monitor the EEI and assess the effectiveness of climate mitigation efforts. This also highlights the need for alternative ways of measuring EEI like the inventory approach proposed in this project.

2.4. Feedback Mechanisms and Climate Sensitivity

The Earth's climate system is governed by feedback that either stabilises or amplifies the effects of radiative forcing modulating the EEI. The five key feedback mechanisms are:

1. Planck Feedback (Negative): Warmer temperatures increase outgoing longwave radiation, stabilizing the system.
2. Water Vapor Feedback (Positive): Rising temperatures increase atmospheric water vapor, enhancing the greenhouse effect.
3. Lapse Rate Feedback (Positive or Negative): Changes in the vertical temperature profile of the atmosphere affect radiative emissions.
4. Surface Albedo Feedback (Positive): Melting ice and snow reduce reflectivity, increasing solar absorption
5. Cloud Feedback (Positive or Negative): Cloud cover changes and cloud properties changes impact both reflection of solar radiation and trapping of infrared radiation.

The combined effect of these feedbacks is quantified by the global climate feedback parameter (λ), measured in $\text{W/m}^2/\text{K}$. This parameter links the radiative forcing (RF) of GHGs to changes in global surface temperature (TAS) via the equation Equation 1:

$$RF_{GHG} + \lambda TAS = EEI \quad \text{Equation 1}$$

The climate sensitivity — how much global temperatures rise for a doubling of CO_2 — is inversely related to λ . While these metrics are essential for predicting future climate change, significant uncertainties remain, especially in the quantification of feedbacks like cloud responses, water vapor dynamics, and the role of aerosols (Forster et al., 2021; Rugenstein et al., 2023).

2.5. Scientific Challenges Ahead

Despite significant progress, major scientific challenges persist in understanding and predicting the Earth's water-energy cycle:

- Precision in Energy Flux Measurements: Can we determine Earth's energy fluxes within a few tenths of W/m^2 , matching the amplitude of climate change (given by the amplitude of EEI), using global observations?
- Consistency Across Datasets: Are current energy cycle datasets consistent enough to close the global energy budget with confidence within a few tenth of W/m^2 ?
- Quantifying the EEI: Can we accurately measure the small EEI ($0.5\text{--}1 \text{ W/m}^2$) with uncertainties as low as $\pm 0.3 \text{ W/m}^2$ on decadal timescales to track changes caused by GHG emissions?
- Quantifying the trend in EEI: Can we accurately measure the small trend in EEI ($0.5\text{--}1 \text{ W/m}^2$) with uncertainties as low as $\pm 0.2 \text{ W/m}^2$ per decade and evaluate the cause for it (changes in the forcing? changes in the feedbacks? both? What is the role of anthropogenic GHG emissions?)?
- Feedbacks and Climate Sensitivity: Can we improve estimates of λ and climate sensitivity to reduce uncertainties in future warming projections?
- Geographic Patterns of Warming: How do surface warming patterns, particularly in polar and tropical regions, influence feedback mechanisms, EEI changes and climate sensitivity?
- Interconnection of the energy cycle with the water Cycle: How can the relationships between the energy cycle and water cycle be better quantified to advance predictive capabilities?
- Modeling Advances: Can we represent critical processes of the water energy cycle like clouds, and convection which interact with the energy cycle to improve climate model simulations of the Earth's water-energy cycle?
- Long-term Monitoring Systems: How can we ensure the continuity of satellite observations and develop complementary missions to avoid data gaps in EEI and TAS?

2.6. Conclusion

Achieving a quantitative understanding of the climate feedback responses to radiative changes necessitates a foundation of precise, comprehensive and globally consistent observations of the water-energy cycle of the Earth. This includes observations of the key water and energy fluxes with a precision of a few tenth of W/m^2 , along with observations of surface air temperature and sea surface temperature with a precision of a few tenth of K at global and regional scale. This project builds on precise satellite observations to derive EEI and TAS to further constrain the global energy budget and estimate the energy fluxes at the level of a few tenth of W/m^2 . The results will then be used to refine estimates of the global climate feedback parameter and the climate sensitivity including their changes with time over the past 2 decades.

3. Requirements for the Earth Energy Imbalance (EEI)

The scientific requirements for the EEI are outlined in Hakuba et al. (2024), which is the most recent review on EEI estimates. Additionally, it is a comprehensive assessment conducted by the global climate community under the framework of the World Climate Research Programme's EEI assessment project of GEWEX (cf <https://www.gewex-eei.org> for more details). Hakuba et al. (2024) summarizes all recent findings on EEI estimates from the climate community and addresses key issues identified regarding EEI estimates derived from different approaches, as discussed in the ESA/WCRP workshop of 2023 (see Final report accessible at the following [link](#)). This section provides a summary of the paper and the requirements in Table 3.

3.1. Summary of Hakuba et al. (2024)

Earth's energy imbalance (EEI) is a fundamental metric for tracking change in Earth's climate and is also a target value in global climate model tuning. The Global Energy and Water Exchanges (GEWEX) community met in spring 2023 at a joint WCRP-ESA EEI assessment workshop to discuss discrepancies and inconsistencies in EEI estimates. This paper intercompared 21 ocean heat content (OHC) time series from various sources and institutions, as well as OHU trends and OHU correlations with CERES net radiative flux variability.

The study showed a significant spread in central OHU estimates (normalised to Earth's TOA surface area) ranging from 0.51 to 0.74 W m⁻² for in situ-based estimates, generally larger values from satellite-based OHC (0.89 W m⁻²), and 0.40–0.96 W m⁻² across six ocean reanalyses. The in situ-based OHC products do not capture the deep ocean below 2000 m, and an estimate of 0.06±0.04 W m⁻² for deep OHU has been added to be representative of the full ocean column.

Temporal variability in annual mean OHU at both 12- and 6-month increments is compared against CERES EBAF net radiative flux variability (Loeb et al., 2018). It stands out that both satellite based, two reanalyses and the in situ+satellite hybrid products, RFROM and PMEL-combined, exhibit correlations with CERES EBAF net radiative flux of 0.44 or larger, while most of the largely in situ-based OHU series do not agree as well. For the in situ-based OHU fields, quality control choices for the observed data are a critical factor not only in reducing measurement error, but in reducing the representation error, the difference between a point source measurement and the wider spatial area represented in the gridded fields used for the OHU calculations. This also applies to reanalysis products, which rely on external (observations processing centres) and internal quality control procedures.

Deriving OHU from OHC data, and their resulting correlation with CERES, is impacted by assumptions such as the differencing method (e.g., first versus centred differences) and temporal sampling/smoothing (monthly vs. annual vs. low-pass-filtered). A major concern for

satellite-derived OHC products is the adequate knowledge of sea water's expansion efficiency of heat, which acts as a scaling factor for OHU variations and significantly affects the magnitude of internal variability and trend in OHU. There is substantial spread not only in OHU central estimates, but the OHU error bars as well. Estimating EEI via heat inventory analysis is to date the most viable approach to closing the Earth's energy budget and largely possible due to the unprecedented coverage of the ocean by Argo floats and satellite altimetry (Meyssignac et al., 2019).

The study of zonal trends in net radiation with CERES data has revealed several key regions of change across the tropics, subtropics and at high latitudes. The gap impact analysis performed ignores the role of measurement uncertainties and potential shifts between non-overlapping parts of a data record, and requires further investigation to include observing system characteristics. The analysis reveals that gaps of any length (between 1 and 25 months) can have a significant impact on deduced trend magnitude and uncertainty, depending on the location of the gap in the data record. The impact is larger for EEI than OHC trends, given the more linear and robust increase in OHC, while EEI trends are more sensitive to the period considered and the interannual variability that substantially shapes the >20-year EEI record (Hakuba et al. 2024).

3.2. Requirements

The first GEWEX-EEI Assessment Workshop held in spring 2023, yielded requirements that have been touched upon in Hakuba et al. (2024) and are summarized in Table 3.

Table 3 *Science requirements for EEI*

Requirements
Discrepancies among EEI and OHU products, methods and their origin, ought to be systematically assessed and improved upon.
Regional, zonal and basin-scale intercomparisons are recommended to better understand global discrepancies and the impact of differing ocean volumes sampled. With respect to regional geodetic OHC analysis, in-depth assessment of expansion efficiency is required
Best practices to enable apples-to-apples comparison—e.g., sampling considerations, uncertainty quantification, OHU derivation—ought to be established and shared with the community
Beyond improving our knowledge of EEI with existing observations, ensuring seamless continuity of these systems and data products should be a priority, as well as efforts to expand those for improved coverage of the ocean, land and cryosphere (see also von Schuckmann et al., 2023)
Novel techniques ought to be explored to provide independent and direct measurements of EEI at the TOA

Understanding EEI changes and their attribution is as important as the comprehensive quantification and characterization of EEI, its trend and its variability

4. Requirements for the Surface Air Temperature (TAS)

4.1. Introduction: Surface Temperatures

4.1.1. Required form of surface temperature

Surface temperatures are of primary importance to society (affecting food, water, health, infrastructure, etc) and within climate science. In climate science, surface temperature responds to and feeds back on climate forcing. To make analyses of climate sensitivity tractable, a key assumption is that major climate feedbacks are significantly related to surface temperature.

More than one “surface temperature” can be defined (Merchant et al., 2013; Figure 1). In this project we use “TAS” to represent surface air temperature generically including land surface air temperature (LSAT) and marine air temperatures (MAT). TAS is (1) sparsely measured by in situ measurement technologies (weather station thermometry, ship air temperature measurements, etc) and (2) is coupled to but not identical to skin temperatures measurable from satellites.

The fundamental science requirement for surface temperature for this project is to obtain: global monthly mean 1-deg resolution surface temperature for 1993 to present, with observational stability sufficient to support analysis of the EEI.

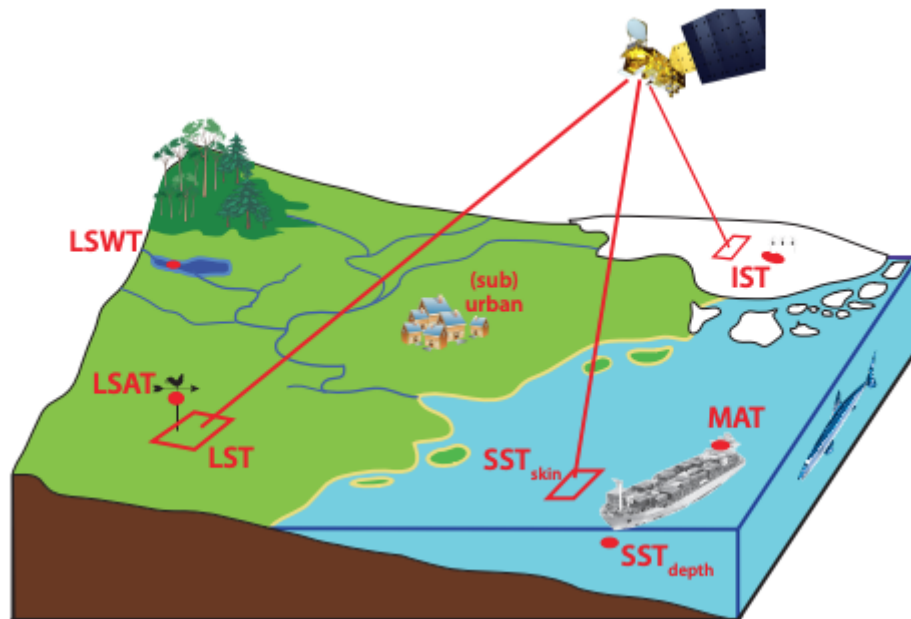


Figure 1 *Different surface temperatures. SST: sea surface temperature, either at depth, measured in situ, or of the skin layer, measured by radiometers on ships or in space; MAT: marine air temperature; LST: land surface temperature, LSAT: land surface air temperature; LSWT: lake surface water temperature; IST: ice surface temperature, which covers land-ice and ice shelves, and SIST for sea-ice surface temperature.*

The approach to be taken is to blend satellite-derived TAS with in situ TAS observations in a global surface temperature analysis. TAS is the most appropriate definition of surface temperature because:

1. TAS is directly measured as in situ air temperature, albeit sparsely
2. it is assumed that TAS is more strongly coupled (through radiative-convective equilibrium) with the mid-tropospheric temperatures that are crucial to climate feedbacks than skin surface temperature

Given the available satellite datasets for skin surface temperature (ST), it is appropriate to verify that TAS rather than skin ST is the more appropriate. This is assessed here by considering the Pearson correlation coefficient between TAS or skin ST and the atmospheric temperature at 500 hPa, using ERA5 reanalysis data. Specifically, the interannual correlation in monthly mean temperatures is calculated for the recent period of sustained anthropogenic global warming, i.e., 1980 to 2024. This is shown for Januarys and Julys in Figure 2.

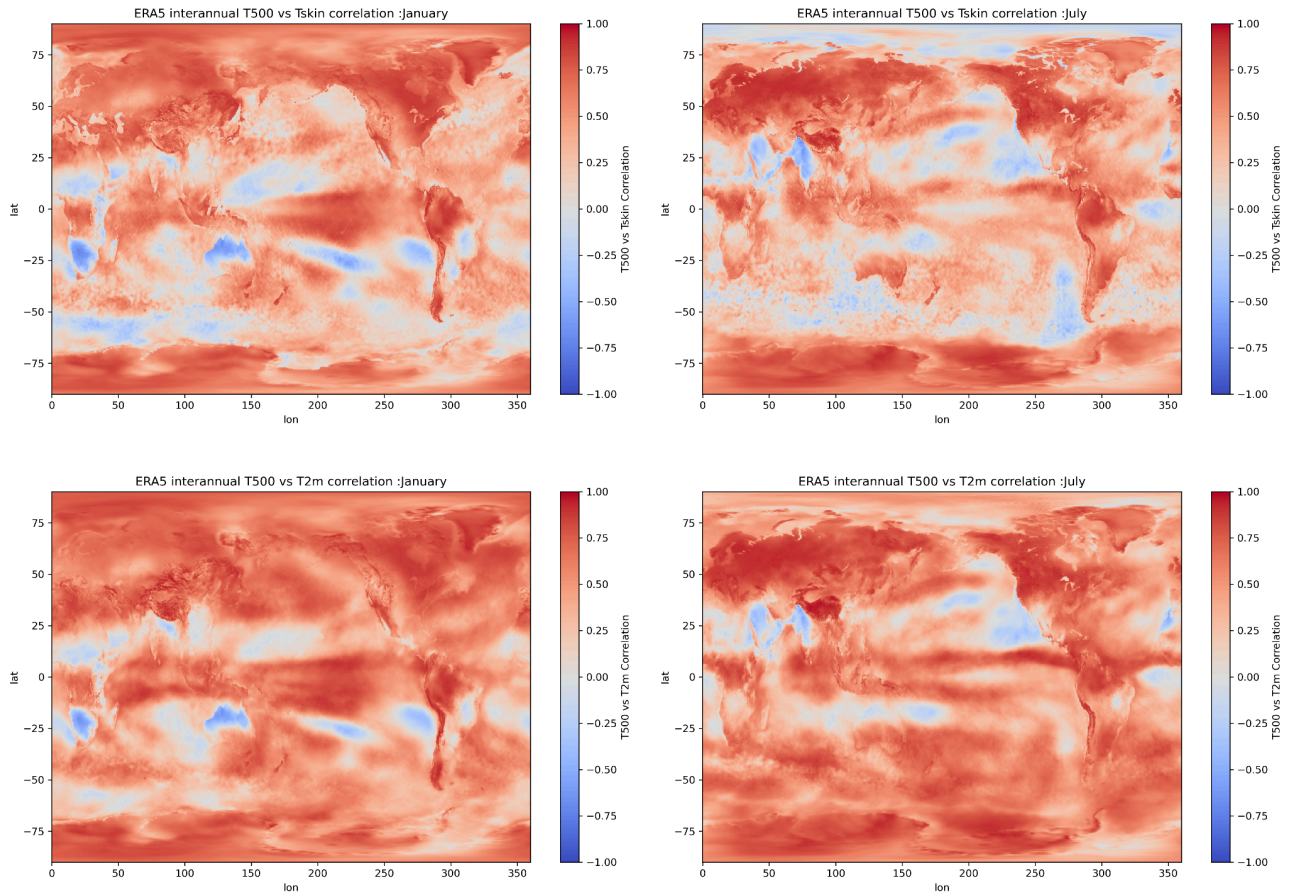


Figure 2 *Correlation coefficient between monthly mean surface temperature and mid-tropospheric temperature (500 hPa) for (left) Januarys and (right) Julys over the period 1980 to 2024. (Upper) correlation of skin ST and mid-tropospheric temperature, and (lower) 2 m air temperature (TAS) and the same.*

Correlation of surface and mid-tropospheric temperature (at 500 hPa) is generally positive, except in areas of climatological atmospheric subsidence (Hadley cell descent), predominantly north and south of the inter-tropical convergence zone. Particularly in mid-latitudes and in the Arctic summer, TAS has a visibly stronger correlation to the middle atmosphere temperature than skin ST, as expected. The area-weighted mean correlation coefficients are not very different (0.48 for skin ST, 0.49 for TAS). Nonetheless, for all latitudes, the TAS correlation is higher (Figure 3).

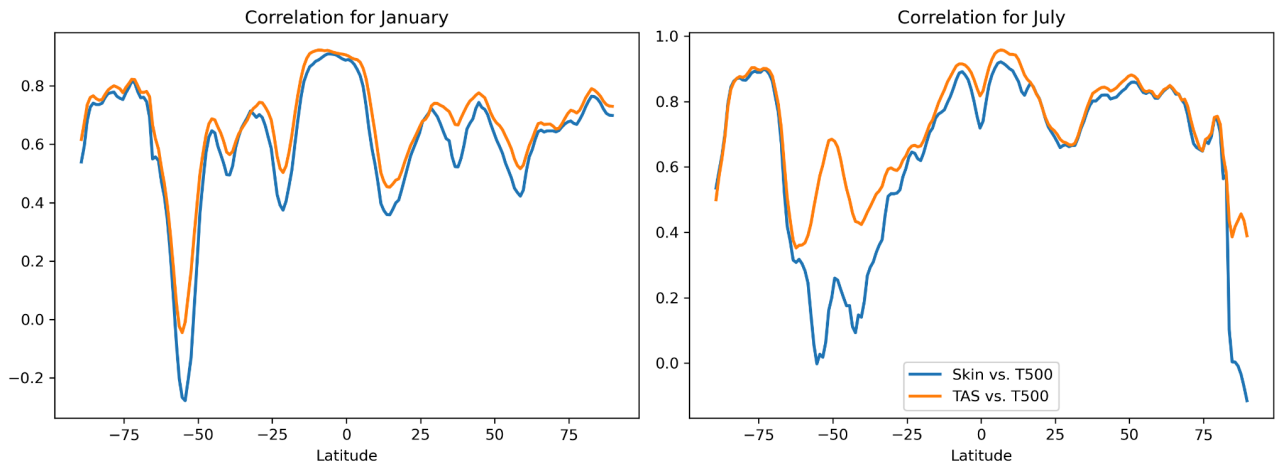


Figure 3 *Correlation between monthly zonal-mean surface and mid-tropospheric temperatures, for Januarys (left) and Julys (right).*

The mid-tropospheric temperature to surface temperature relationship is maintained by convection, and therefore it is possible that the maximum of the daily surface temperature is better correlated with mid-tropospheric temperature than the daily average. After all, deep convection arising over equatorial Africa, for example, is phased to mid-afternoon (e.g., Nowicki and Merchant, 2004).

ERA5 data are available as monthly averages by hour of day. Figure 4 shows the multiyear (1980 - 2024) mean of the maximum of the monthly averages by hour of day ("Tmax") minus the monthly mean (averaged over all hours, "Tmean") of the TAS. There is little difference between Tmax and Tmean in the winter high latitudes and over the oceans in general. Meanwhile, in the mid-troposphere, the equivalent difference is <0.3 K on average, and is significantly more than 2 K only over Tibet, where the high altitude couples the surface and 500 hPa level more closely.

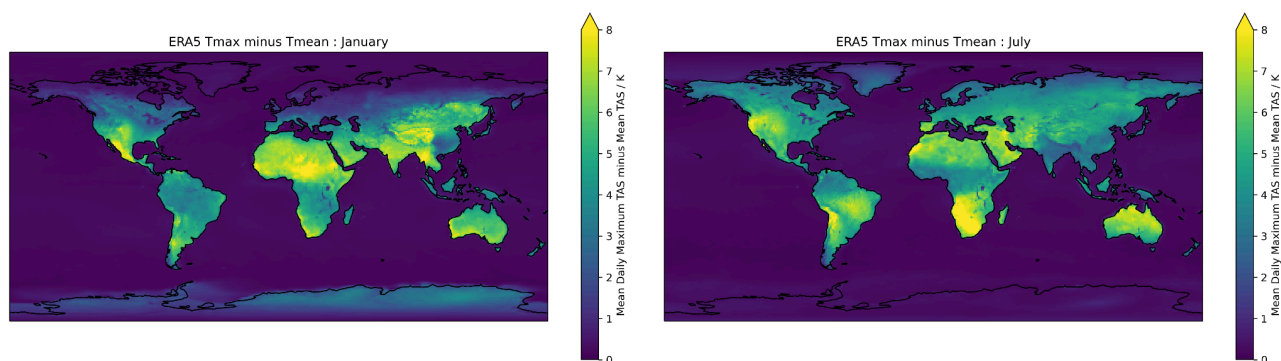


Figure 4 *Mean difference of Tmax from Tmean for (left) January and (right) July.*

Figure 5 shows the correlation using Tmax rather than Tmean to represent TAS, the mean values being 0.46 and 0.47 for January and July. As the correlation coefficients are generally

higher in Figure 2 (lower panels), the use of daily mean TAS is confirmed as the optimum choice.

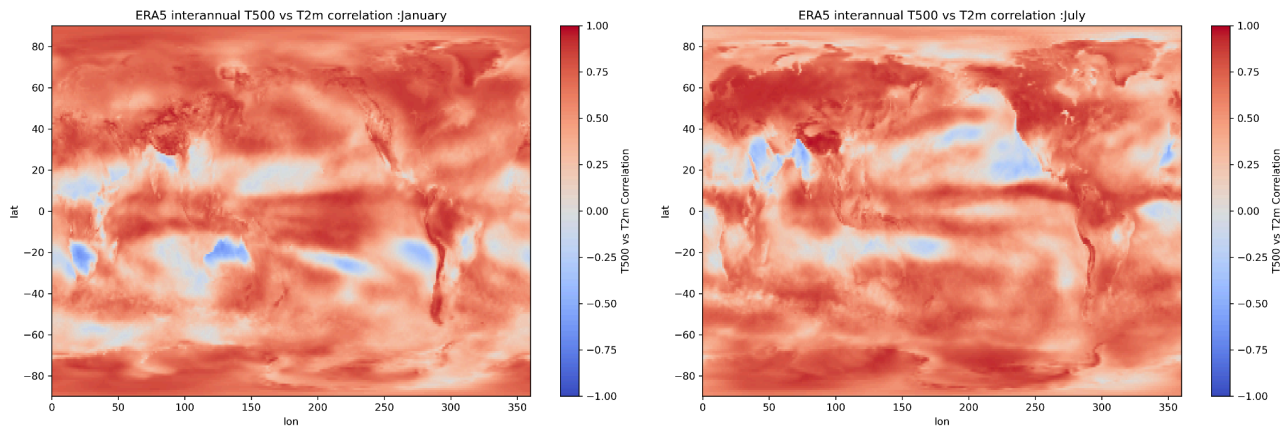


Figure 5 *As Figure 2, but for the T_{max} rather than T_{mean} representation of TAS.*

4.1.2. General requirements on satellite-derived TAS

The scientific requirements below apply to all satellite-derived TAS ("sat-TAS") products that will be used within the MOTECUSOMA analysis. The next section specifies domain-specific further considerations. Note that where a requirement is not yet fully agreed, this provisionality is indicated by "[TBC]" (to be confirmed) is used to indicate a provisional statement of requirement.

1. Sat-TAS products shall be obtained at daily 0.25° latitude-longitude resolution, which is computationally feasible and supported from previous experience in the EUSTACE project. This is required to reduce the spatiotemporal representativity errors that may arise in the monthly 1° TAS data for climate analysis from clear-sky satellite sampling.
2. Sat-TAS data shall be made by building relationships between satellite and TAS measurements (not precluding use of additional inputs and analyses), accounting for all major sources of variability in these relationships on monthly 1° (and longer/larger) scales.
3. The definition of the target TAS quantity represented by the relationships shall be daily mean 2 m air temperature. (Where the feasible TAS quantity differs in detail from that target definition, uncertainty and the potential for systematic trends arising from the definitional difference shall be estimated.)
4. The dominant effects causing sat-TAS uncertainty shall be separately characterised in terms of the uncertainty each contributes, and, where relevant, each effect's spatial and temporal error-correlation length scales.
5. Uncertainty shall be quantified for each sat-TAS datum for each of the important effects separately (so that correlation length scales can be accounted for in analysis).
6. A sat-TAS product derived for a particular domain shall include data only for locations where that domain is valid as per the project TAS-team common grid definition.
7. Satellite surface temperature to sat-TAS relationships shall by design estimate any trends of decadal variability in skin-TAS differences (i.e., will not merely track the satellite skin temperature if geophysical variability means that skin-air differences

change on monthly 1° (and longer/larger) timescales. This addresses the issue of sat-TAS observational stability.

4.2. Science Requirements for Marine TAS

4.2.1. Open-ocean marine air temperature

This subsection identifies specific scientific requirements for the generation of products of daily 2 m air temperature estimates (i.e. "sat-TAS") at daily/0.25 degree cells across the open ocean, including the Caspian Sea, including cells with fractional sea ice cover(section 4.2.2).

The SST-TAS relationship over the open-ocean will be derived using Monin-Obukov boundary layer similarity theory via bulk formulae (Biri et al., 2023). These formulae provide estimates of the stability of the atmosphere using a limited set of meteorological variables: as a minimum SST, wind speed and TAS are required. Statistical distributions for the joint variability of these values will be derived from the L4 CCI data, ERA5 and ship-based measurements respectively. These relationships are expected to be conditional on wind direction derived from the ERA5 U and V vectors. Humidity may be a useful additional variable , and the sensitivity of the results to inclusion of those data will be tested.

Following the approach taken in the TAS analysis system ([section 4.4](#)) the open-ocean SST-AT conversion will proceed in two stages:

- 1) Distributions of stability estimates that are conditional on wind speed will be formed and used to adjust the SST temperature (t_0) to 2m as:

$$t_2 = t_0 + \frac{t^*}{k} \left(\ln \frac{2}{z_{0t}} - \Psi_t \left(\frac{2}{L} \right) \right) \quad \text{Equation 2}$$

- 2) *In situ* MAT values at the respective observing heights (z) will be adjusted to 2m as:

$$t_2 = t_z + \frac{t^*}{k} \left(\ln \frac{z_t}{2} - \Psi_t \left(\frac{z_t}{L} \right) + \Psi_t \left(\frac{2}{L} \right) \right) \quad \text{Equation 3}$$

Equation 2 and Equation 3 represent respectively a bottom-up and top-down approach to the height adjustment, where $k=0.4$ (von Karman constant), t^* , z_{0t} and L are respectively the scaling parameter, roughness length and Monin-Obukov length. Monin-Obukov similarity theory includes the assumptions that near surface vertical gradients in the atmosphere are the result of turbulence and that upstream conditions are sufficiently homogeneous. If either of these conditions are not met, for example in very stable conditions or near oceanic fronts, then uncertainty in the estimates will be increased, and will be estimated. Ψ_t is the temperature stability function, which varies depending on the parameterization chosen. Several different parameterizations can be used, but these will produce different stability estimates and hence height adjustments. The differences will be largest under very high or very low wind speeds. The effect of parameterization choice on the sat-TAS estimates will be investigated using several parameterizations that are included in the AirSeaFluxCode package (Biri et al., 2023).

This package includes 10 parameterisations, some suitable for use with bulk SST data and some, like that used by ECMWF, with skin SST. Following Biri et al. (2023) the uncertainty that arises from the parametrization choice will be determined, using estimates of the bulk-skin temperature difference from ERA5 where required.

Uncertainty in the sat-TAS estimates (in both processing stages) that arise from the different parameterizations is likely to have a complex structure, and it is not currently known how this interacts with the other components of the uncertainty budget. This will be investigated but simplifications will likely be necessary.

The nature of the conditional distributions in stage 1 will need to be decided. Wind direction will likely be an important component for determining the sat-TAS relationship because of the effect on air temperature from the upwind temperatures, but this is not directly used in the bulk formulae. As such, experiments will be conducted to determine the effect of including this variable as a conditional parameter in the stability distributions.

In stage 2 of the processing, in situ MAT data will be taken from the NOC-developed reprocessing of the ICOADS dataset. Observation heights (z in Equation 2) will be taken from the WMO Pub 47/OCEANOPS metadata catalogue. Missing height values, with suitable uncertainty estimates, will be completed after Kent et al. (2013) and Cornes et al. (2020). Uncertainty in the height adjustment will likely follow the example used in Morice et al. (2024), with an ensemble of realizations that combine stability and height uncertainty being provided. A suitable ensemble size will be decided through communication with the TAS analysis developers.

Additional uncertainty elements for the ship MAT data will follow the example of Cornes et al. (2020) and will consist of uncorrelated random and conditionally common components. The conditionally common component will be evaluated per ship and per year, with propagation to the analysis system via an error covariance matrix.

Ship-based MAT values generally suffer from a diurnal heating bias that results from energy storage by the superstructure of the ship. The traditional approach to this has been to exclude daytime values and restrict the sample to those values recorded at night. A correction for this bias was developed by Cropper et al. (2023) and will be applied in this analysis to enable daytime values to be used, thus expanding the available sample by a factor approaching two. The heating bias correction removes the full diurnal cycle to give nighttime-equivalent values. It will be necessary therefore to explore approaches to reconciling the nighttime-equivalent values with the required daily averages and to estimate the uncertainty in the adjustment. The uncertainty structure in the daytime heating adjustment will follow Cropper et al. (2023) and Morice et al. (2024) and will be propagated via the error covariance matrix.

A key science requirement is understanding the representation uncertainty that arises from the different effective spatial/temporal resolution of the gridded data and ship observations, and how those uncertainties propagate to the L4 analysis. The ship MAT data represent instantaneous (time and space) values. Hence the SST will need to be at the highest resolution possible (0.05 deg / daily) and co-located to the ship data. Understanding the most suitable resolution for the conditional-distributions in stage 1 needs to be decided, particularly with regards to the propagation to the larger spatial/temporal scales (0.25 daily) and then monthly L4 analysis.

4.2.2. Air temperature over high sea-ice concentrations

This subsection identifies specific scientific requirements for the generation of products of daily 2 m air temperature estimates (i.e. "sat-TAS") from the Global L4 Sea and Sea Surface Temperature (SST/IST) CDR of C3S. This is a daily gap-free satellite surface temperature product at 0.05 degree resolution that provides IST (ice surface skin temperature) in regions where sea ice is present in concentrations greater than 70%.

This sat-TAS product will be an input to the daily 0.25 degree analysis, and shall be provided as a L4 daily file, including values only for the 0.25 degree cells within the project-agreed ocean domain where IST is present in the 0.05 degree product. The fraction of the 0.05 degree cells within the 0.25 degree cell that contributed ISTs to the sat-TAS will also be provided as metadata.

The conversion of the IST to daily mean sat-TAS shall be achieved by relationships built in using matched satellite and in situ data from numerous drifting ice stations and buoys, e.g. from NP, CRREL, and those distributed from ECMWF (TBC by KO+12). The relationships established shall account for the following factors:

- the wind speed and direction via the impact on the turbulent heat fluxes and skin-T2m differences
- the control that cloud cover exerts on skin-T2m differences
- Insufficient representation of the diurnal cycle in the daily ISTs (to be mitigated by training against all-sky in situ data e.g. in case of seasonal dependencies in the sampling)

The following factors shall not be directly accounted for:

- Leads and areas of ice where concentration is <70%
- Changes in albedo over time on any timescales, which can affect the surface energy balance and therefore the T2m-Tskin relationship.

The relationships used to convert satellite input data to sat-TAS shall use the following auxiliary data and externally defined parameters:

- surface wind speed from ERA5 cloud cover information from L3 mask and ERA5

The dominant sources of uncertainty ("effects") in the sat-TAS values are expected to be the following:

- Satellite data effect - the propagation of uncertainty in the satellite input data through the conversion relationship. The TAS uncertainties are probably on the order of the satellite uncertainties (e.g. 1-2 K) but systematic biases in the satellite data may be removed in the relationship building due to the training against in situ observations.
- Sampling effect - the propagation of uncertainty from representativity errors in the satellite input data due irregular overpassing times during the day and to not making retrievals in the infrared where clouds are present
- In situ effect - the propagation of uncertainty in the in situ station input data through the conversion relationship

- Representation effect - due to the limited in situ data availability to train and test the models, these models will be tuned towards the regions and times with observations, which may not represent all conditions. The lack of representative in situ data in time and space might lead to a bias in the relationships relative to the "truth best" relationship
- Mask effect - the uncertainty in the classification of the sea ice region
- Fitting effect - the relationship uncertainty characterised by the residuals in the fitted relationship
- Auxiliary data effect -- uncertainty arising from errors in auxiliary data set that bias the relationships
- Point to pixel effect - This effect will be treated as a random effect.

A method for estimating the uncertainty (standard deviation of the estimated error distribution) for each of the above effects and the corresponding spatio-temporal correlation characteristics shall be developed as part of the relationship building work. We would expect some of these effects to be correlated, such as the uncertainty between one in situ observation and another. We expect that the main source of uncertainty will be from the representation effect, due to very limited in situ observations in particular over the Antarctic sea ice. Another dominant source of uncertainty will likely be the sampling uncertainty as a result of residual cloud contamination.

4.2.3. Marginal ice zones: sea-ice/water mixtures

This subsection identifies specific scientific requirements for the generation of products of daily 2 m air temperature estimates (i.e. "sat-TAS") from the Global L4 Sea and Sea Surface Temperature (SST/IST) CDR of C3S. This is a daily gap-free satellite surface temperature product at 0.05 degree resolution that provides MIZT (marginal ice surface temperature) in regions where sea ice concentration is between 15 and 70%.

This sat-TAS product will be an input to the daily 0.25 degree analysis, and shall be provided as L4 daily files. The fraction of the 0.05 degree cells within the 0.25 degree cell that contributed MIZTs to the sat-TAS will also be provided as an additional "n" variable.

The conversion of the satellite MIZT input data to daily mean sat-TAS shall be achieved by relationships built in using matchups between the MIZT data and in situ near surface air temperature (T2m) measurements. Generally, there are very few in situ observations of MIZT and efforts will be put into collecting, quality controlling and analysing in situ observations (from Sail-drones, UpTempo buoys and possibly other sources) to evaluate their potential for the relationship building. . The relationships established shall account for the following factors:

- the wind speed and direction via the impact on the turbulent heat fluxes and skin-T2m differences
- the control that cloud cover exerts on skin-T2m differences
- Insufficient representation of the diurnal cycle in the daily ISTs (to be mitigated by training against all-sky in situ data e.g. in case of seasonal dependencies in the sampling)

The following factors shall not be directly accounted for:

- Sea ice drift within a day. Sea ice can have a very complex nature and can drift significantly within a day. The T2m conversion differs from sea ice to open ocean but

accurate sea ice drift products are not available to be used to account for this effect. It is anticipated that this effect will introduce random uncertainties.

The relationships used to convert the satellite MIZT input data to sat-TAS shall use the following auxiliary data and externally defined parameters:

- Wind speed and direction from ERA5
- Cloud cover information from L3 and ERA5

The dominant sources of uncertainty ("effects") in the sat-TAS values are expected to be the following:

- Representation effect - due to the limited in situ data availability to train and test the models, these models will be tuned towards the regions and times with observations, which may not represent all conditions. The lack of representative in situ data in time and space, which might lead to a bias in the relationships relative to the "truth best" relationship
- Satellite data effect - the propagation of uncertainty in the satellite input data through the conversion relationship. The TAS uncertainties are probably on the order of the satellite uncertainties (e.g. 1-2 K) but systematic biases in the satellite data may be removed in the relationship building due to the training against in situ observations.
- Sampling effect - the propagation of uncertainty from representativity errors in the satellite input data due irregular overpassing times during the day and to not making retrievals in the infrared where clouds are present
- In situ effect - the propagation of uncertainty in the in situ station input data into the obtained satellite-TAS relationship
- Mask effect - the uncertainty in the classification of the marginal ice zone
- Fitting effect - the relationship uncertainty characterised by the residuals in the fitted relationship

A method for estimating the uncertainty (standard deviation of the estimated error distribution) for each of the above effects and the corresponding spatio-temporal correlation characteristics shall be developed as part of the relationship building work. We expect that the main sources of uncertainty will arise from the representation effect, due to very limited in situ observations in the marginal ice zone and the classification of the marginal ice zone (i.e. the mask effect).

4.3. Science Requirements for Land TAS

4.3.1. Surface air temperature over land and lakes

This subsection identifies specific scientific requirements for the generation of products of daily 2 m air temperature estimates (i.e. "sat-TAS") from daily day-and-night separately clear-sky satellite LST products from LST_cci at 0.01 deg resolution over areas designated as land, lakes (with the exception of the Caspian Sea), and all snow and ice-covered surfaces over land including glaciers. Over the Greenland and Antarctic Ice Sheets the relationships will be derived as for other surfaces over land, but the output results will be replaced by those built in

Section 4.3.2. The sat-TAS estimates will be of daily mean TAS, i.e., the relationships built will include accounting for the diurnal cycle.

From these 0.01 deg day-and-night daily-mean L3 outputs, the sat-TAS product required for the analysis will be calculated. This shall be provided as L3 files of daily mean at 0.25 degrees, containing daily mean TAS calculated by aggregating (accounting for relative uncertainties) all the 0.01 deg day-and-night TAS estimates.

The conversion of the satellite LST and LSWT input data to daily min and max sat-TAS shall be achieved by relationships built in using matchups between the LST data aggregated to 0.05 degrees (to reduce noise relative to use of 0.01 deg) and in situ land surface air temperature (T2m) measurements from stations, provided by the Global Historical Climatology Network - daily (GHCN-d) dataset. The relationship equations will be built using MODIS data, but the daily min and max sat-TAS data will be built from multiple satellite input data (MODIS, SLSTR, VIIRS, ATSRs). For lakes, there are some publicly available above-water data sets for North American Great Lakes, and we will seek to get permission to augment these with other datasets available to Lake CCI (will be very sparse). The relationships established shall account for the following factors:

- the wind speed and humidity via the impact on the turbulent heat fluxes and skin-T2m differences
- the control that cloud cover exerts on skin-T2m differences
- the land cover class and vegetation fraction through the impact of surface roughness on the skin-T2m differences
- the snow cover impact on skin-T2m differences
- the effect of elevation on skin-T2m differences
- diurnal cycle

The following factors shall not be directly accounted for:

- Temperature range effect - the uncertainty in the representation of Tmax and Tmin equivalents in the LST data across the whole globe. This is because the peaks and troughs of the LST diurnal cycle are different in local time depending on the biome, climate class and geolocation. The relationships will attempt to account for this but extremes may have a greater uncertainty that may not be adequately estimated.

The relationships used to convert the satellite LST and LSWT input data to sat-TAS shall use the following auxiliary data and externally defined parameters:

- Wind speed, dew point temperature and air temperature from ERA5, with relative humidity derived.
- Land cover class (biome) originally sourced from Land Cover CCI, fractional vegetation from Copernicus Global Land Service, solar zenith angle, and snow cover originally sourced from the Ice mapping System (IMS) of the National Snow and Ice data Center (NSIDC). All of these are accompanying variables within the LST_cci LST datafiles.
- Digital Elevation Model from Copernicus

The dominant sources of uncertainty ("effects") in the sat-TAS values are expected to be the following:

- Satellite data effect - the propagation of uncertainty in the satellite input data through the conversion relationship
- Sampling effect - the propagation of sampling uncertainty in the satellite input data due to clouds. These uncertainties are estimated in the LST_cci products and available to be propagated through to the relationships.
- Surface type effect -- the various uncertainties in the auxiliary data sets, i.e. from the snow cover, land cover class, fractional vegetation, wind speed, relative humidity, DEM. The uncertainties for snow cover, land cover class, and fractional vegetation are estimated in the LST_cci products and available to be propagated through to the relationships. The effects due to wind speed, relative humidity and DEM are additional ingested during the relationship building.
- Station effect - the propagation of uncertainty in the in situ station input data through the conversion relationship, which is an effect injected during the relationship building.
- Mask effect - a fixed land-sea mask is used, but in some areas the variability of the land-sea boundary is significant
- Fitting effect - the relationship uncertainty characterised by the residuals in the fitted relationship

A method for estimating the uncertainty (standard deviation of the estimated error distribution) for each of the above effects and the corresponding spatio-temporal correlation characteristics shall be developed as part of the relationship building work. We would expect some of these effects to be correlated, such as the error between one station and another. The surface type effects will have correlation length scales in time and space which will need to be analysed. It is anticipated that the spatial length scale for these would be dependent on land cover class within climate zones. The temporal scale can be of the order of days to weeks, and itself is seasonally dependent. A dominant source of uncertainty will likely be the sampling uncertainty as a result of residual cloud contamination.

4.3.2. Surface air temperature over ice sheets and shelves

This subsection identifies specific scientific requirements for the generation of products of daily 2 m air temperature estimates (i.e. "sat-TAS") from daily L4 satellite IST products covering the Greenland and Antarctic ice sheets and the Antarctic ice shelves at 0.01 deg resolution. Other ice and snow-covered surfaces over land including glaciers will be covered by the relationships built in Section 4.3.1.

This sat-TAS product will be an input to the daily 0.25 degree analysis, and shall be provided as L4 daily files. A fixed ice-sheet domain will be used, which is an approximation.

The conversion of the satellite IST input data to daily mean sat-TAS shall be achieved by relationships built in using matchups between the IST data and in situ near surface air temperature (T2m) measurements from stations provided by PROMICE, GC-NET and AMRC (TBC by KO + 12). The relationships established shall account for the following factors:

- the wind speed and direction via the impact on the turbulent heat fluxes and skin-T2m differences
- the control that cloud cover exerts on skin-T2m differences
- the effect of elevation on skin-T2m differences

- Insufficient representation of the diurnal cycle in the daily ISTs (to be mitigated by training against all-sky in situ data e.g. in case of seasonal dependencies in the sampling)

The following factors shall not be directly accounted for:

- Due to the lack of in situ observations it is not possible to derive a separate relationship model for the Antarctic ice shelves, and the sat-TAS over the ice shelves will be derived by using the relationship of the Antarctic ice sheet. Any truth differences in the relationships due to the different surface types (ice sheet vs ice shelves) will not be accounted for.
- Changes in albedo over time, which can affect the surface energy balance and therefore the T2m-Tskin relationship

The relationships used to convert the satellite IST input data to sat-TAS shall use the following auxiliary data and externally defined parameters:

- Wind speed and direction from ERA5
- Cloud cover information from L3 and ERA5
- Digital Elevation Model from Copernicus

The dominant sources of uncertainty ("effects") in the sat-TAS values are expected to be the following:

- Satellite data effect - the propagation of uncertainty in the satellite input data through the conversion relationship. The TAS uncertainties are probably on the order of the satellite uncertainties (e.g. 1-2 K) but systematic biases in the satellite data may be removed in the relationship building due to the training against in situ observations.

Sampling effect - the propagation of uncertainty from representativity errors sampling uncertainty in the satellite input data due irregular overpassing times during the day and to not making retrievals in the infrared where clouds are present

- Representation effect - due to the limited in situ data availability to train and test the models, these models will be tuned towards the regions (e.g. the margins of the Greenland ice Sheet) and times with observations, which may not represent all conditions. The lack of representative in situ data in time and space, which might lead to a bias in the relationships relative to the "truth best" relationship.
- In situ effect - the propagation of uncertainty in the in situ station input data through the conversion relationship
- Mask effect - the uncertainty in the classification of the ice sheet and ice shelves boundaries
- Fitting effect - the relationship uncertainty characterised by the residuals in the fitted relationship
- Auxiliary data effect -- uncertainty arising from errors in auxiliary data set that bias the relationships
- Point to pixel effect - This effect will be treated as a random effect. The influence from sloping terrain may introduce systematic effects but these are likely small.

A method for estimating the uncertainty (standard deviation of the estimated error distribution) for each of the above effects and the corresponding spatio-temporal correlation characteristics shall be developed as part of the relationship building work. We expect that the main uncertainties will arise from representation effects, due to the limited availability of in situ data in particular in the Southern hemisphere, and the sampling effect as a result of residual cloud contamination.

4.4. Science Requirements for TAS Analysis

The TAS analysis system includes two processing stages:

1. Production of L3 non-interpolated air temperature estimates from satellite derived surface temperature observations for domains specified in Section 4.3. This includes propagation of uncertainty associated with input observation data and quantification of uncertainty in the surface to air temperature conversion process.
2. Production of a global L4 interpolated analysis that merges satellite air temperature estimates, from (1) with in situ air temperature observations, with quantified uncertainties.

4.4.1. Single domain L3 non-interpolated TAS estimates

Single domain L3 air temperature estimates will be produced by applying surface temperature to air temperature conversion methods for which requirements are described in [Section 4.3](#) of this report. A central component of this task is propagation of uncertainty, e.g. following end-to-end uncertainty propagation as in Mittaz et al. (2019), a scheme which also allows for “injected” uncertainty arising in the assumptions behind any transformation as well as traditionally “propagated” terms. This should include:

- Propagation of uncertainty associated with the input satellite surface temperature retrievals used and representativity of the satellite sampling.
- Propagation of uncertainty associated with surface temperature to air conversion -, propagated from uncertainty in parameters and injected by approximations and assumptions.

Critically, non-independent error structures in observations need to be specified to allow the subsequent L4 merged analysis to account for the heterogenous range of observation sources used. This requires representation of:

- Uncertainty for errors with systematic structure between observations (e.g. as a function of the sensor, or of another auxiliary variable, or requiring communication of a more complex error model).
- Uncertainty for errors defined by a non-zero and non-unity correlation between observations (e.g. with specified uncertainty magnitudes and spatial or temporal correlation decay functions/parameters).
- Uncertainty associated with errors that are independent between observations, including that associated with incomplete sampling at the provided L3 grid resolution.

This requires two-way communication between TAS observation data providers, specifying uncertainty in satellite air temperature retrievals, and developers of the L4 analysis, specifying the range of uncertainty structures that can be accommodated in the L4 analysis. This will

allow the merged L4 analysis to account for the heterogeneous range of observation sources to be merged.

4.4.2. Merged multi-domain L4 interpolated TAS estimates

Recent interpolated near-surface temperature analyses based on in situ data have included assessments of uncertainty associated with systematic errors that are propagated into analysis fields and derived climate diagnostics (e.g. Huang et al., 2020; Lenssen et al., 2024; Morice et al., 2021). Application of end-to-end uncertainty propagation for satellite earth observation is challenging due to the intrinsically large data volumes associated with EO data. Uncertainty estimates in interpolated L4 satellite surface temperature products typically account for uncertainty interpolation while neglecting uncertainty related to systematic observation error structures (e.g. Merchant et al., 2019; Nielsen-Englyst et al., 2023).

A framework for uncertainty propagation for systematic observation errors into a combined in situ and satellite surface air temperature L4 analysis was developed within the EUSTACE project (Rayner et al., 2020), based on computationally efficient spatial statistical methods (Lindgren et al., 2011). The EUSTACE interpolated analysis data set used a simplified observation error model with a partial representation of systematic observation error structures. MONTECUSOMA will build on the EUSTACE L4 analysis approach for a more complete propagation of uncertainty for systematic effects into its analysis fields.

The L4 analysis methods will be based on a statistical model of air temperature variability, providing interpolation through a model of covariance of air temperature fields. Production of the interpolated air temperature estimates requires:

- Specification of this model structure to include specification of climatological and covariate information, as it is expected to use auxiliary climatological information from ERA5 as a first guess to be updated from MOTECUSOMA TAS estimates.
- Fitting of regional/seasonal model parameters to represent regional variability in TAS.
- Appropriate representation of uncertainties in satellite L3 TAS estimates agreed with the developers of surface temperature to TAS relationships, including communication of any required approximations in uncertainty modelling, e.g. arising from computational or modelling limitations..
- Specification of uncertainty models for in situ observations of land and marine TAS.

End of the document